Local Electrodynamics in Heavy Ion Irradiated $Bi_2Sr_2CaCu_2O_{8+\delta}$

R. A. Doyle,[1,2] W. S. Seow,[1] Y. Yan,[1] A. M. Campbell,[1] T. Mochiku,[3] K. Kadowaki,[3,4] and G. Wirth[5]

[1]*Interdisciplinary Research Centre in Superconductivity, University of Cambridge, Cambridge, CB3 0HE, England*
[2]*Department of Condensed Matter Physics, Weizmann Institute of Science, Rehovot 76100, Israel*
[3]*National Research Institute for Metals, 1-2-1, Sengen, Tsukuba, Ibaraki 305, Japan*
[4]*Institute of Materials Science, The University of Tsukuba, 1-1-1, Tenodai, Tsukuba, Ibaraki 305, Japan*
[5]*Gesellschaft fur Schwerionenforschung, Planckstrasse 1, D-4291, Darmstadt, Germany*
(Received 17 April 1996)

Transport measurements in the flux transformer and c-axis geometries are used to investigate vortex dynamics in heavy ion irradiated BSCCO crystals. In the flux transformer geometry there is a range of fields, temperatures, and angles where the primary and secondary voltages show close correspondence, as observed in YBCO. This occurs because the columnar defects suppress thermal fluctuations and decrease ρ_c. Values for ρ_{ab} and ρ_c are extracted from the flux transformer data assuming local anisotropic electrodynamics and compared with directly measured c-axis data. Good agreement confirms the validity of local resistivity. This is supported by both measurement configurations indicating that ρ_c vanishes faster than ρ_{ab}. [S0031-9007(96)00874-5]

PACS numbers: 74.60.Ge, 74.60.Jg

Measurements in the flux transformer (FT) geometry are a useful means of probing the dimensionality or longitudinal correlation of vortices in the liquid state in both $Bi_2Sr_2CaCu_2O_{8+\delta}$ (BSCCO) [1–3] and $YBa_2Cu_3O_{7-\delta}$ (YBCO) [4–8]. However, the difficulties associated with interpretation of data measured in the quasiforce free configuration have been discussed in detail by Brandt [9]. Reported FT data indicate that the entire vortex liquid state in BSCCO is 2D [1–3] since flux cutting always generates a sizable voltage drop along the c axis in the linear resistivity regime. Thus the primary voltage V_p is always much larger than the secondary voltage V_s. On the other hand, the resistive transition in the FT geometry in (twinned) YBCO [10] apparently proceeds via two steps. V_p and V_s appear at almost the same temperature and show close correspondence over a small range of temperatures. This implies that ρ_{ab} is measurable before ρ_c and is claimed to result in a "disentangled" or 3D vortex liquid. At some higher thickness dependent temperature, longitudinal correlation is also lost and ρ_c becomes measurable at the onset of an "entangled liquid." Entanglement should, however, not be confused with flux cutting which is what causes the c-axis dissipation and results in a difference between V_p and V_s. Subsequently, it has been shown [11] that close correlation of the voltages in the FT geometry in YBCO only occurs in the presence of twin boundaries, a type of correlated disorder. In clean YBCO crystals, correlation is lost in all directions simultaneously at what is suggested to be a first order phase transition [12]. Recent measurements on BSCCO also suggest that the melting transition [13,14] involves a loss of c-axis correlation [15].

Despite the large anisotropy of BSCCO there are indications that vortices in heavy ion irradiated (HII) BSCCO behave as lines rather than independent stacks of pancakes [16,17]. This is associated with the topological corre-spondence between the columnar defects induced by the HII and the stacks of pancake vortices. Static magnetization measurements (of the vortex solid) show uniaxial enhancement of the irreversibility line when the magnetic field is applied parallel to the columnar defects [16,18]. Seow *et al.* [17] have found similar enhancement in HII BSCCO using transport measurements (which probe the liquid state).

Possible nonlocal effects in the electrodynamic behavior of the vortex liquid should be directly related to the vortex dimensionality. The finite line tension of a vortex can, under certain conditions, induce a voltage distantly from the position where (nonuniform) currents act on it: precisely the situation which is probed by the FT geometry. Safar *et al.* [4] found evidence for nonlocal behavior in twinned YBCO crystals using this method. Their conclusions are based on differences between the apparent ratios $\rho_{ab}/\rho_c(T)$ determined from FT and direct c-axis configurations. The effect was explained using a phenomenological hydrodynamic theory of a viscous vortex liquid by Huse and Majumdar [19]. Eltsev and Rapp, on the other hand [6,8], using similar crystals and parameters to Safar *et al.* [4], satisfactorily explained their data using local theory. Measurements on BSCCO by Busch *et al.* [1] also showed that their data were described well by local electrodynamics. This is less surprising since, in as-produced BSCCO, the stacks of pancake vortices have a vanishingly small line tension. The recent data suggesting a finite line tension is apparent for vortices in HII BSCCO [16–18] are supported by theoretical considerations which indicate that such defects increase the c-axis correlation by suppressing thermal fluctuations of pancake vortices [20]. This suggests that nonlocal effects similar to those apparently observed in the more 3D YBCO system [4] might be observed in HII BSCCO, and this is the subject of this paper.

Samples of BSCCO were grown in an infrared furnace [21]. Both surfaces of the selected crystals were optically smooth. Four 25 μm gold wires were attached to each (ab-plane) surface in the FT geometry. Contact resistances are less than 4 Ω for each pair. The configuration is shown in the inset in Fig. 1. Two crystals were measured. Crystal K1 has dimensions of $1.04 \times 0.41 \times 0.01$ mm while crystal K2 has dimensions of $1.03 \times 0.52 \times 0.01$ mm. The electrode spacing is $\Delta_x \approx 0.25$ mm. Reliability of the FT data is carefully screened by checking the symmetry when current is injected from each side of the crystal. Measurements were made using a lock-in amplifier and low noise transformer at a frequency of 72.8 Hz and current of 2 mA. This current is well within the linear resistance regime for all temperatures. This was verified by measuring all configurations at currents between 0.1 and 10 mA as well as making dc IV measurements. Nonlinear effects appear above 6 mA, where heating effects cannot be precluded. The crystals were irradiated at GSI Darmstadt, with a 2.25 GeV Au ion beam aligned close to the c axes. We define matching fields, B_Φ, where the vortex spacing $a_0 \approx (\Phi_0/B)^{1/2}$ is equal to the average defect spacing d. Crystal K1 was irradiated to $B_\Phi = 0.5$ T and K2 to $B_\Phi = 2.0$ T. Transmission electron microscopy studies show that the irradiation induces continuous columnar defects with radius $b_0 \approx 3.5$ nm.

We begin with the qualitative features of FT data for irradiated BSCCO. Figure 1 presents $V_p = V_{23}(I_{14})$ and $V_s = V_{67}(I_{14})$ for crystal K1. Remarkable reentrant behavior is exhibited by V_s at all fields shown below and slightly above the matching field. V_p and V_s show close correspondence in a region above where they vanish for fields below B_Φ. The amplitude of the peak in V_s grows with field, shows a maximum between 60 and 70 K, and disappears above 1.3 T for crystal K1 ($B_\Phi = 0.5$ T) and above 3 T for K2 ($B_\Phi = 2.0$ T). No such peaks in V_s were observed before irradiation. Much smaller peaks of a qualitatively different nature become apparent in V_s at high currents (≈ 10 mA) before irradiation, as reported

elsewhere [1,3]. These latter peaks, which are dependent on the current amplitude [3], disappear below the sensitivity at temperatures well above V_p. The peaks seen in Fig. 1 closely resemble those observed in deoxygenated [22] twinned YBCO crystals and are associated with the correlated disorder. For $B > B_\Phi$, interstitial vortices dominate the behavior similar to as-produced BSCCO. Interaction between the vortices in different layers becomes weaker than intralayer interactions so that the reentrant V_s disappears.

Figure 2 presents a phase diagram constructed from the FT data in Fig. 1. It indicates $T_{\mathrm{irr}}(B)$, where V_p disappears below the resolution. This line crosses ($B_\Phi = 0.5$ T) close to $T^* \approx 69$ K, where vortex localization on the columnar defects is expected in BSCCO [20]. There is a rapid drop in the pinning ability of the defects at a temperature, T_l, where the thermal energy becomes comparable to the pinning energy. This occurs for sample K1 just below 80 K in agreement with other data [18]. The inset of Fig. 2 shows the angular dependence of V_p and V_s at 72.8 K for crystal K1 at 0.5 T as the magnetic field is rotated through alignment with the columnar defects. The peak in V_s extends to 60° to 70° from the c axis, consistent with other reports [23,24]. The dip near $\theta = 0$ is the direction of the irradiation. There is also a small angular range where V_p and V_s show correspondence. From the results of Fig. 1, we calculate the value of ρ_c assuming local electrodynamics. We use the anisotropic approximation based on the Laplace equation following Busch *et al.* [1] and calculate $(\rho_c/\rho_{ab})^{1/2} = (L/\pi t)\mathrm{arccosh}(V_p/V_s)$ and $(\rho_c\rho_{ab})^{1/2} = V_p L/I\pi(\Delta_x)$, where Δ_x is the electrode spacing and w the crystal width. The resistivity components can then be separated. By injecting current along the c axis, ρ_c can also be obtained from $V_c = V_{27}(I_{18})$ and $\rho_c^d = V_c L w/It$, where I is the current, L the length, w the crystal width, and t the thickness. This "direct" measurement assumes uniform current flow along the c axis and is usually justified over a large range of temperatures because of the extreme resistive anisotropy ($\gamma^2 = \rho_c/\rho_{ab} = 170^2$) which means
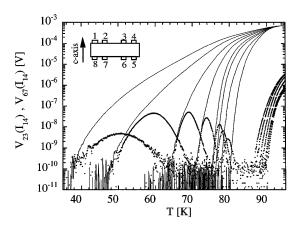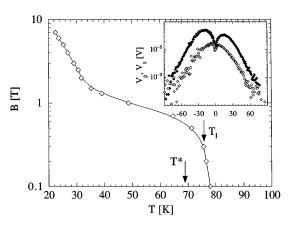

FIG. 1. Primary, $V_{23}(I_{14})$ (solid line), and secondary, $V_{67}(I_{14})$ (points), voltages for crystal K1 for $B//c//$defects of 0.1, 0.2, 0.3, 0.5, 0.7, 1.0, and 1.3 T. $B_\Phi = 0.5$ T. The inset shows the contact configuration.

FIG. 2. The field dependence of the T_{irr}, where V_p vanishes for crystal K1. The line is a guide, and the temperatures T^* and T_l are discussed in the text. The inset shows $V_p(\theta)$ and $V_s(\theta)$ at 72.8 K and 0.5 T. $\theta = 0$ corresponds to $B//$defects.

the crystal is effectively "stretched" along the c axis by a factor of 170. This results in an "isotropic" c-axis dimension of about 2 mm, as compared to the electrode spacing which is 10 times smaller. The values of $\rho_c(T)$ from both methods are presented for different fields in an Arrhenius plot in Fig. 3. Very satisfactory agreement is apparent. We have also used V_p, together with the directly measured ρ_c, to recalculate V_s to see whether this would correctly reproduce the remarkable reentrant peak. This result is shown for crystal K1 in Fig. 4 at 1.0 T for $B//c$, also yielding satisfactory agreement. Figure 5 shows the angular dependence of the extracted resistivity components from the data in the inset of Fig. 2. Both ρ_c and ρ_{ab} show a cusp for $B//$defects.

In unirradiated BSCCO crystals, the anisotropy is sufficiently large at all temperatures that V_s shows a weak peak [1] or does not reappear at all before V_p disappears below the sensitivity [2]. This means there is a large voltage drop along the c axis wherever the primary voltage is measurable. Whenever there is a current component parallel to the field, as there is in all these measurements, flux cutting of some kind must occur to produce a voltage component along the direction of the field [9].

This is well known in conventional superconductors, where the flux structure in the force free configuration can be extremely complex and the J_c nonlocal [25]. In 2D systems with weak pinning, flux cutting is very easy [26]. Then the external field can be regarded separately from the flux rings produced by the self-field of the (c-axis component of the) current. The system is linear, and local anisotropy theory can be used [1]. On the other hand, in irradiated crystals, strong pinning is introduced and ρ_c is dramatically reduced in the mixed state for $B//$defects [17]. We understand the data as follows. In an applied field, $\rho_{ab}(T)$ decreases monotonically with temperature. However, ρ_c displays a pronounced maximum so that the anisotropy, $\gamma^2 = \rho_c/\rho_{ab}$, also shows a maximum. In the FT geometry, the current is injected into one face only and penetrates the crystal to a distance $z_{\rm eff} = $

$L\pi^{-1}(\rho_{ab}/\rho_c)^{1/2}$, where L is the length of the crystal [1]. Clearly the maximum in ρ_c corresponds to a minimum in $z_{\rm eff}$. The value we estimate is about 1 μm, considerably smaller than the crystal thickness. Since V_s is sensitively determined by the proximity of the current to the bottom electrodes, it results in V_s dropping below the noise level close to but below T_c. At lower temperatures, ρ_c falls much faster than ρ_{ab} in HII BSCCO, reducing the effective anisotropy. Thus $z_{\rm eff}$ is increased, and V_s reappears in the vortex liquid state as shown in Fig. 1. What is more important is that V_s approaches and shows close correspondence with V_p in a small window of temperatures before both disappear, as also seen in the much more 3D YBCO system [4–7]. This implies ρ_c has dropped to a very small value, an effect which indicates a strong enhancement in the correlation of vortices in the vortex liquid. The columnar defects effectively increase the interlayer coupling by suppressing thermal fluctuations of pancake positions. Our observations are also in agreement with previous studies showing that even weak random pinning strongly suppresses the helical instabilities which result in flux cutting in the force free configuration [9].

Next we consider the validity of local electrodynamics to the behavior of the samples studied. There is a clear qualitative resemblance of the data in Fig. 1 to that in twinned YBCO where nonlocal effects were inferred [4]. There are two ways in which nonlocality can be established. One is to show a thickness dependence in ρ_c itself. The other way is to show that local theory does not work. However, the results in Fig. 3 suggest that ρ_c is accurately recalculated by local theory. The curves are all smooth functions, suggesting a uniform resistive mechanism at all temperatures. A stronger test of locality is consistency between the apparent ratios of ρ_c/ρ_{ab} extracted from local theory from the two geometries where the current is injected parallel and perpendicular to the ab planes [4]. The inset in Fig. 3 shows the temperature dependence of the ratios, $V_{67}/V_{23}(I_{14})$ and $V_{36}/V_{27}(I_{18})$, for crystal K1 at 0.5 T.
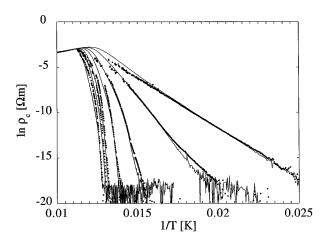
FIG. 3. Directly measured ρ_c extracted from $V_{27}(I_{18})$ (solid lines) and from the FT data (points) as discussed in the text for the same fields as in Fig. 1.
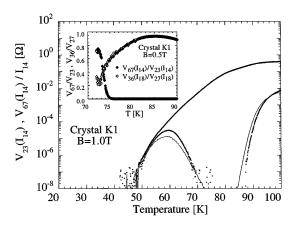
FIG. 4. Primary $V_p(T)/I$ and secondary $V_s(T)/I$ apparent resistances (points), and calculated secondary apparent resistance from the primary and c-axis voltages (solid line) for crystal K1 at 1.0 T. The inset shows the temperature dependence of the ratios V_{67}/V_{23} and V_{37}/V_{26} at 0.5 T for crystal K1.
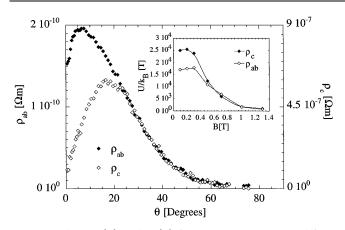
FIG. 5. The $\rho_{ab}(\theta)$ and $\rho_c(\theta)$ for K1 at 0.5 T extracted from the inset in Fig. 2. The inset shows U_{eff}^{ab} and U_{eff}^c determined from ρ_{ab} and ρ_c extracted from the FT data.

When current is injected in the top face and ρ_c drops more rapidly than ρ_{ab}, $V_{67}/V_{23}(I_{14})$ should approach unity, as it indeed does. Accordingly, $V_{36}/V_{27}(I_{18})$ should approach zero in a local scenario since the current shrinks away from the voltage electrodes before ρ_{ab} vanishes. In both crystals, V_{36} disappears before V_{27}, resulting in a ratio which approaches zero. These data imply the validity of local electrodynamics in irradiated BSCCO crystals. We cannot entirely preclude the possibility that nonlocal effects might affect ρ_c in the same way for both geometries, thereby allowing the local theory to be used. However, the consistency of the data makes this seem unlikely. Therefore we suggest that the close correspondence between V_p and V_s arises not because of nonlocal effects but because ρ_c becomes small (in a narrow range of angles for $B//$defects) and z_{eff} approaches the crystal thickness, resulting in an almost uniform Lorentz force. Similar current redistribution effects were invoked [27] to explain a simultaneous peak in V_s and minimum in ρ_c for $B//ab$ planes in BSCCO crystals.

Finally, the evidence supporting an enhanced c-axis correlation is briefly discussed. The angular dependence of the extracted resistivities shown in Fig. 5 shows that both components are reduced for $B//$defects, as expected for strong uniaxial pinning and a finite line tension. Well away from alignment, the (scaled) resistivity reverts to the 2D behavior that is observed in unirradiated crystals. The apparent activation energies U_{eff} determined from ρ_c and ρ_{ab} (from the FT data) are shown for crystal K1 in the inset in Fig. 5. These are obtained by a linear fit by Arrhenius plots between 10^{-4} and 10^{-6} of $\rho(100 \text{ K})$. The absolute values are about an order of magnitude greater than those obtained from equilibrium magnetization measurements [28]. However, overestimation of U_{eff} from resistance measurements is well known due to its temperature dependence [29]. Therefore we concentrate only on the field dependence. U_{eff} is almost independent of field below B_Φ, suggesting that the vortices are indeed localized on the defects. Above B_Φ there is close agreement between U_{eff}^{ab} and U_{eff}^c. This is consistent with unirradi-

ated BSCCO [30] and also with the scaling of $\rho_c(\theta)$ and $\rho_{ab}(\theta)$ when the angle between the field and defects is large. It may be understood by consideration of similar origins of dissipation for the resistivity components. In weakly coupled layered superconductors, one mechanism determining both resistivity components is thermal activation of pancake vortices away from pins. This affects ρ_{ab} in the usual way through the Lorentz force and may be connected to ρ_c through induced phase slips between the Josephson coupled layers. Alternatively, this can be explained by decoupling of the planes, allowing pancakes associated with interstitial vortices to become mobile.

In conclusion, we have shown that correlated disorder in the form of columnar defects modifies the effective anisotropy in the vortex liquid state in BSCCO. This results from strong uniaxial pinning apparent for fields parallel to the defects. Our data are consistent with an anisotropic local resistivity even though there is a clear increase in the c-axis correlation due to the defects.

[1] R. Busch *et al.,* Phys. Rev. Lett. **69**, 522 (1992).
[2] H. Safar *et al.,* Phys. Rev. B **46**, 14 238 (1992).
[3] Y. M. Wan *et al.,* Phys. Rev. Lett. **71**, 157 (1993).
[4] H. Safar *et al.,* Phys. Rev. Lett. **72**, 1272 (1994).
[5] F. de la Cruz *et al.,* Philos. Mag. B **70**, 773 (1994).
[6] Yu. Eltsev, W. Holm, and Ö. Rapp, Phys. Rev. B **49**, 12 333 (1994).
[7] Yu. Eltsev and Ö. Rapp, Phys. Rev. B **51**, 9419 (1995).
[8] Yu. Eltsev and Ö. Rapp, Phys. Rev. Lett. **75**, 2446 (1995).
[9] E. H. Brandt, Rep. Prog. Mod. Phys. **58**, 1465 (1995).
[10] D. Lopez *et al.,* Phys. Rev. B. **50**, 7219 (1994).
[11] D. Lopez *et al.* (unpublished).
[12] W. Kwok *et al.,* Phys. Rev. Lett. **72**, 1088 (1994).
[13] E. Zeldov *et al.,* Nature (London) **375**, 373 (1995).
[14] D. Fuchs *et al.* (unpublished).
[15] R. A. Doyle *et al.,* Phys. Rev. Lett. **75**, 4520 (1995).
[16] L. Klein *et al.,* Phys. Rev. B **48**, 3523 (1993).
[17] W. S. Seow *et al.,* Phys. Rev. B **53**, 14 611 (1996).
[18] D. Zech *et al.,* Phys. Rev. B **52**, 6913 (1995).
[19] D. A. Huse and S. N. Majumdar, Phys. Rev. Lett. **71**, 2473 (1993).
[20] A. Koshelev, P. Le Doussal, and V. M. Vinokur (unpublished).
[21] T. Mochiku and K. Kadowaki, Trans. Mater. Res. Soc. Jpn. **19A**, 349 (1993).
[22] D. Lopez *et al.* (to be published).
[23] R. C. Budhani, W. L. Holstein, and M. Suenaga, Phys. Rev. Lett. **72**, 566 (1994).
[24] C. J. van der Beek *et al.,* Phys. Rev. Lett. **74**, 1214 (1995).
[25] J. R. Cave, Philos. Mag. B **37**, 111 (1978).
[26] D. Kumar *et al.,* J. Appl. Phys. **76**, 2361 (1994).
[27] V. N. Zavaritsky, Physica (Amsterdam) **235C**, 2715 (1994).
[28] C. J. van der Beek *et al.* (unpublished).
[29] E. Zeldov *et al.,* Appl. Phys. Lett. **56**, 680 (1990).
[30] A. E. Koshelev, Phys. Rev. Lett. **76**, 831 (1996).